Environmental Nanotechnology, Monitoring & Management 3 (2015) 1–9

Environmental Nanotechnology, Monitoring & Management

journal homepage: www.elsevier.com/locate/enmm

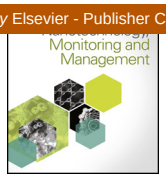

Adsorption of Mn (II) ion on polyvinyl alcohol/chitosan dry blending from aqueous solution

Z. Abdeen [a,*], S.G. Mohammad [b], M.S. Mahmoud [c]

[a] Petrochemical Department, Egyptian Petroleum Research Institute, Nasr City, Cairo, Egypt
[b] Central Agricultural Pesticides Laboratory, Pesticide Residues and Environmental Pollution Department, Agriculture Research Center, Dokki, Giza 12618, Egypt
[c] Sanitary and Environmental Institute (SEI), Housing and Building National Research Center (HBRC), Egypt

ARTICLE INFO

Article history:
Received 7 June 2014
Received in revised form
22 September 2014
Accepted 28 October 2014
Piero Gardinali

Keywords:
Mn (II) biosorption
PVA/CS dry blending
Thermodynamic

ABSTRACT

The present study explored the ability of polyvinyl alcohol/chitosan (PVA/CS) binary dry blend as an adsorbent for removal of Mn (II) ion from aqueous solution. We will study how the solid-state shear ball milling is employed to prepare the polyvinyl alcohol/chitosan hydrogel crosslinked without using the crosslinking agent. The PVA/CS was characterized by LDS, X-ray diffraction, FTIR and SEM. The results revealed that during the process of ball milling at ambient temperature, a PVA/CS blending can be effectively pulverized resulting in crosslinking of PVA/CS hydrogel having nanosized particles. Also, the removal of Mn (II) ion has been found to be pH, adsorbent dosage and contact time dependent and the optimum pH was 6.0. From the testing of equilibrium data by Langmuir and Freundlich isotherm models, it was found that the adsorption equilibrium was fitted well by Freundlich isotherm model. In addition, the kinetic adsorption was fitted well by the pseudo-second-order kinetic model. The thermodynamic study indicated that the adsorption of Mn (II) ion onto PVA/CS was spontaneous and endothermic in nature. Also, it showed that the PVA/CS binary blend was a good adsorbent for the removal of Mn (II) ion from aqueous solution.

1. Introduction

Toxicities of water sources due to the discharging of industrial effluents is a worldwide environmental problem. Industrial wastewater often contains a considerable amount of heavy metal ions and organic pollutants, which would endanger to public health and the environment. Heavy metals are generally introduced into the environment through natural phenomena and human activities (Abollino et al., 2003). The contamination of the existing water resources is increasing day by day with industrialization. The disposal of wastewater containing heavy metal ions is always a challenging task for environmentalists (Ngah et al., 2002).

Removal of heavy metals from wastewater is a very important factor with respect to human health and environmental considerations (Nourbakhsh et al., 2002). Manganese polluted water is annoying in all respects, since the appearance, color, taste and odor are affected. At low concentration, it stains everything and it comes in contact with including fabrics. The recommended limit in drinking water is 0.05 mg/L and between 0.01 and 0.02 mg/L in water meant for industrial purposes. It has been implicated for neurological disorder when inhaled at a rate of about 10 mg day^{-1} (Adeogun et al., 2011); thus, there is a need for effective removal of Mn (II) from its aqueous solution.

The use of potentially low-cost sorbents to remove heavy metals from aqueous solutions has been intensely studied (Bailey et al., 1999). For instance, chitosan, extracted from crustacean shells, is a biopolymer with the capacity to fix a large variety of heavy metals due to its relatively high proportion of active nitrogen sites (Muzzarelli, 1977). The waste shrimp shell, the raw material to produce chitin and chitosan constitutes approximately 40–50% of the total weight (Xu et al., 2008).

The adsorption process also depends on the physicochemical characteristics of the aqueous solutions, such as pH, redox potential, temperature, the concentration and speciation of metallic ions and the presence of other ions (cations or anions) in the aquatic system.

Blending is an important process for developing industrial applications of polymeric materials, and compatibility among components has a marked influence on the resulting physical properties of polymer blends (Folkes and Hope, 1985).

Poly (vinyl alcohol) (PVA) is a water-soluble material containing large amounts of hydroxyl groups, non-toxic, biocompatible, cheap and chemically stable. PVA has been widely applied because it has

* Corresponding author. Tel.: +20 2 22736349; fax: +20 2 22747433.
E-mail address: ziziabdeen@yahoo.com (Z. Abdeen).

http://dx.doi.org/10.1016/j.enmm.2014.10.001

many advantages such as low cost, non-toxicity, biocompatibility, high durability and chemical stability (Khoo and Ting, 2001; Kao et al., 2009). Several studies on the PVA/chitosan blend films have been reported. According to Miya and Iwamoto (1984) chitosan forms a clear homogeneous blend with PVA and the tensile strength of the blend is greater than the component values.

Ball milling is a well-known method for generating nanostructured systems and for inducing solid-state reactions, including inorganic synthesis and mechanical alloying (Tan et al., 2004; Kong et al., 2002; Zaluski et al., 1995). The mechanical treatment can also lead to disorder in the material, phase transformations and the formation of solid solutions.

In this article, PVA/chitosan blend hydrogel (semisynthetic hydrogel) (Abdeen, 2011) was prepared using ball milling method because it is a simple, safe and an economic method. The aim of this study is using potentially low-cost sorbents prepared by binary blending of poly (vinyl alcohol) with chitosan having nanosized particles in the absence of crosslinking agent. The potential use of poly (vinyl alcohol)/chitosan having nanosized particles as alternative adsorbent for the removal of Mn (II) ion from aqueous solutions was also investigated. Also, the q_{max} value of the prepared PVA/CS adsorbent will be compared with those of other adsorbents (Yahya et al., 2014; Vijayaraghavan et al., 2011; Üçer et al., 2006). The effects of various parameters, viz. pH, adsorbent dose, initial metal ion concentration, and contact time on the biosorption capacity, were investigated. Different isotherm models were applied to the experimental data. Kinetic and thermodynamic adsorptions were also investigated and reported.

2. Materials and methods

2.1. Chemicals

The PVA used in this study was of analytical grade and was purchased from Merck, Germany. The average Mwt of the PVA was 127,000 and the degree of hydrolysis was 89%. The shrimp shells were collected from seafood shops and washed under running water to remove soluble organics, adherent proteins and other impurities. Then it was dried in an oven at 70 °C for 24 h or longer until completely dried shells were obtained. Hydrochloric acid, oxalic acid, potassium permanganates, potassium hydroxide and sodium hydroxide were purchased from Merck, Germany, and were used without further purification.

2.2. Preparation of chitosan

The chitinous material (shells of the shrimp) was decalcificated with 1.0 M HCl (3.0%, w/v) at room temperature with constant stirring for 1.5 h. The decalcified product was filtered, washed and dried, and then deproteinized with 4% NaOH solution at 50 °C with constant stirring for 5 h. The deproteinized chitin was filtered and washed with de-ionized distilled water until the pH became neutral. It was dehydrated twice with methanol, and once with acetone, and dried. The dried chitin was added to boiling 0.1% potassium permanganate solution to remove the odor and to 15% oxalic acid solution to remove the color. The product chitin was filtered, washed with distilled water and dried. The chitosan was prepared by adding the dried chitin into a three-necked flask containing a solution of 40% (w/v) KOH. It was refluxed under a nitrogen atmosphere at 135–140 °C for 2 h (Abdeen, 2005). The deacetylated chitin (chitosan) was filtered, washed with distilled water, and dried, Fig. 1.

2.3. Preparation of polyvinyl alcohol/chitosan binary dry blend hydrogel

Poly (vinyl alcohol)/chitosan binary blend powder hydrogel was prepared by mixing of equal amounts of poly (vinyl alcohol) and chitosan in the ratio 1:1. The blending was milled by ball milling (Reech, PM400, Germany) for 8 h and 350 rpm at ambient temperature (Tan et al., 2004).

2.4. Preparation of metal ion solutions

The metal ion solution was prepared from analytical grade chemical (Merck Ltd.). A stock solution of 1000 mg/L of Mn (II) was prepared from $MnSO_4{\cdot}H_2O$ in double distilled water. The working solutions were prepared from the stock solutions by diluting it to appropriate volumes. The initial pH of the working solution was adjusted to 5.0 by adding 0.1 N HNO_3 or 0.1 N NaOH solutions and was measured using a JENWAY pH-Meter 3305.

2.5. Biosorption experiments

Batch adsorption experiments were carried out at room temperature (30 ± 1 °C). Adsorption experiments were conducted at different conditions, viz. contact time (5–120 min), pH (1–7), initial Mn (II) ion concentration (5–100 mg/L), and polyvinyl alcohol/chitosan (PVA/CS) dose (0.1–1 g/100 ml). The adsorbent dose was maintained at 0.8 g/100 ml std. solution. The mixtures were taken in a 250-ml conical flask and agitated on a mechanical shaker. The samples were filtered after analysis through Whatman 40 filter paper. The concentrations of metal ion were determined by using atomic absorption spectrophotometer (ICE 3000 Series AA Spectrometer – Thermo Scientific) at 279.5 nm analytical wavelengths. Experimental analysis was repeated. The amount of metal ion adsorbed by the biosorbent at equilibrium (q_e, mg/g) was calculated as follows:

$$q_e = \frac{(C_0 - C_e)V}{m} \quad (1)$$

where V is the volume of solution treated in ml, C_0 is the initial concentration of metal ion in mg/L, C_e is the equilibrium metal ion concentration in mg/L, and m is the biomass in grams.

The percent removal (%) of metal ion was calculated using the following equation:

$$\text{Removal}\,(\%) = \frac{C_0 - C_e}{C_0} \times 100 \quad (2)$$

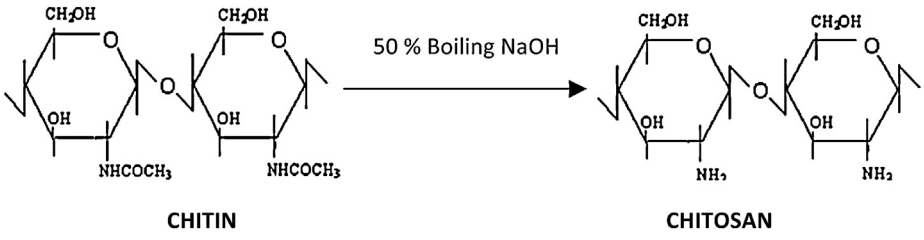

Fig. 1. The preparation of chitosan by deacetylation of chitin.

2.6. Biomass characterization

2.6.1. Fourier transform infrared spectroscopy (FTIR)

The structure and morphology of PVA/chitosan were characterized by using the Fourier transform infrared spectroscopy (FTIR) to identifying characteristic surface functional groups on the adsorbent which in some cases are responsible for the binding of the adsorbate molecules. The spectrum was recorded from 4000 to 400/cm adopting the KBr pellet method of sample handling.

2.6.2. Degree of deacetylation

Infrared spectra were measured by an Ati Mattson FTIR spectrophotometer. The deacetylated chitin (chitosan) CS was subjected to infrared spectroscopy to calculate the degree of deacetylation (D.D.)%, by the relationship:

$$\text{D.D.} = 100 - \left[\frac{(A1660/A3450) \times 100}{1.33}\right] (\%), \quad (3)$$

where A = absolute height of the absorption band of the amide group and a hydroxyl group respectively (Mima et al., 1983).

2.6.3. Molecular weight determination

Molecular weight is also one of the significant characteristics that control the functional properties of CS. Viscosity is one of the simplest techniques that is widely used for estimation of the molecular weights of polymers. The viscosity-average molecular weight was calculated using Mark–Houwink equation relating to intrinsic viscosity (McKay et al., 1987).

$$[\eta] = K_m M v a \quad (4)$$

where $K_m = 8.93 \times 10^{-4}$ and $a = 0.716$ at 25 °C are the empirical Viscometer constants that are specific for a given polymer, solvent and temperature.

2.6.4. Degree of swelling

Swelling is the most significant characteristic of hydrogels and it reflects the affinity of the chemical structure of hydrogels for water and other surrounding fluids. A known weight of the polyvinyl alcohol/chitosan blending powder was immersed in solutions of different pHs (5, 7) at 25 °C until the swelling equilibrium was reached. The powder was removed by filtration and dried with absorbent paper to get rid of excess water and then weighed. The degree of swelling of this sample was calculated with the following equation:

$$DS = \frac{m - m'}{m'} \quad (5)$$

where m and m' denote the weights of the sample and dried sample, respectively (Ferrus and Pages, 1977).

2.6.5. X-ray diffraction measurements

XRD patterns were obtained on Siemens (Berlin, Germany) D500 diffractometer with a back monochromator and a Cu anticathode.

2.6.6. Scanning electron microscopy

Phase morphology was studied using a JSM-T20 (JEOL, Tokyo, Japan) scanning electron microscope (SEM). For scanning electron observations, the surface of the sample was mounted on a standard specimen stub. A thin coating ($\sim 10^{-6}$ m) of gold was deposited into the sample surface and attached to the stub prior to SEM examination in the microscope to avoid electrostatic charging during examination.

2.6.7. Dynamic light scattering (DLS)

The average particle size and size distribution of polyvinyl alcohol/chitosan blending powder were determined by dynamic light scattering (DLS) using a Zetasizer Nano ZS instrument (Malvern, UK). The DLS measurements were performed with an angle of 170° by using a He–Ne laser (4 mW) operated at 633 nm. In brief, 1 mg/ml of nanoparticulate suspension was prepared in double distilled water and sonicated for 30 min. Then, 0.1 ml of the above NPs suspension was diluted to 1 ml in water and then subjected to particle size measurement.

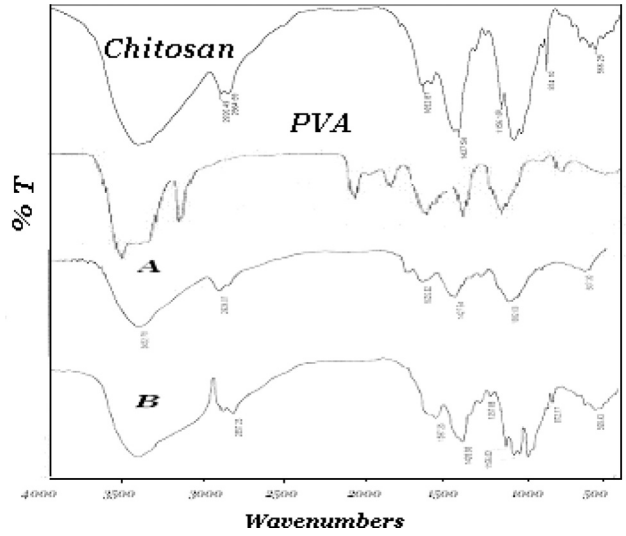

Fig. 2. IR spectra of chitosan, PVA, PVA/chitosan before (A) and after adsorption (B).

3. Results and discussion

3.1. Hydrogel crosslinked network

Different methods of crosslinking have been used in hydrogel formulations. Generally physical and chemical methods have been applied commonly. In chemically crosslinked hydrogels, crosslinking can be produced by covalent bonds between different polymer chains, while in physically crosslinked hydrogels, physical interactions exist between different polymer chains which prevent them from dissolution (Hennink and Nostrum, 2002). The interest toward physically crosslinked gels has been increased in recent years due to the elimination of crosslinking agent in these hydrogels (Kumar, 2000). Physically crosslinked hydrogels mainly demands two conditions: (1) inter-chain interactions in the molecular network must be strong enough to form semi-permanent junction points (2). The network must allow the penetration of maximum water molecules inside the polymer network (Berger et al., 2004). In this work the physically crosslinked PVA/CS hydrogels was by dry blending using ball milling, where the inter-chain interactions in the molecular network between the PVA and chitosan chains, occurred.

3.2. Fourier transform infrared spectroscopy (FTIR)

From FTIR analysis shown in Fig. 2, the degree of deacetylation (D.D.) of the prepared chitosan (CS) was calculated and found to be 61.67%. The PVA, chitosan, PVA/chitosan dried blending, its crosslinking, and their structures were assessed by FTIR spectra, as presented in Fig. 2. The spectrum was recorded before (A) and after adsorption (B) of Mn ions for the crosslinked PVA/chitosan to study the effect of adsorption. The stretching frequency at 1150–1130 cm^{-1} indicates the formation of acetal ring by crosslinking. Furthermore, the band at 840 cm^{-1}, assigned to the C—H rocking region of PVA, disappeared from the spectra of the pure chitosan and the PVA/CS 50/50 blend powder. The strong broad band at 3300–3500 cm^{-1} is the characteristic of the N—H and

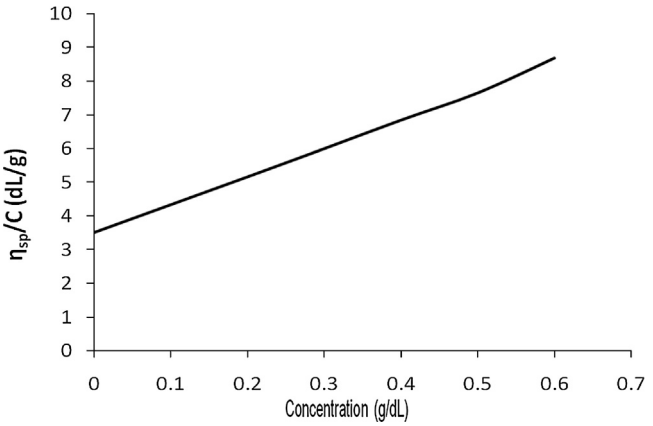

Fig. 3. The reduced viscosity of chitosan versus concentration at 25 °C.

—OH stretching vibration. The significant decrease in transmittance in this band after adsorption of Mn indicated that the bonding of metals with NH_2 group occurred (Jin and Bai, 2002). Thus, the nitrogen atom of chitosan moiety acted as a main adsorption site for Mn adsorption on the crosslinked PVA/chitosan. Also, the FTIR spectra showed that the N—H bending vibrations at 1644 and 1562 cm^{-1} shifted to 1634 and1553 cm^{-1} after the adsorption of Mn, which suggested the interactions between Mn and —NH_2 groups. Since Mn can act as Lewis acid and —NH_2 is a Lewis base, coordination is possible by electron transfer.

3.3. Molecular weight determination of CS

The viscosity-average molecular weight (Mv) of the prepared chitosan sample CS is determined by using an Ostwald Viscometer at 25 °C in 0.3 M acetic acid and 0.2 M sodium acetate buffer solution and was calculated by using Eq. (4). As shown in Fig. 3, the intrinsic viscosity [η] of the prepared chitosan CS sample was 3.5 dL/g and the viscosity-average molecular weight (Mwt) was 99,998 Da.

3.4. Degree of swelling

The PVA and chitosan are water loving in nature and thus have moderate solubility in water with pH 7 without crosslinking, although they have a high swelling degree, Fig. 4. However, after suitable crosslinking they become complete water insoluble material. Water loving nature aroused due to considerable hydrogen bonding with hydrophilic groups. Because of crosslinking, the swelling behavior of PVA/chitosan was also reduced to 44.7% (w/w) at pH 7, as shown in Fig. 4. Thus, the crosslinking is necessary to enhance the chemical stability of PVA/chitosan in acidic medium, pH 5, Fig. 4.

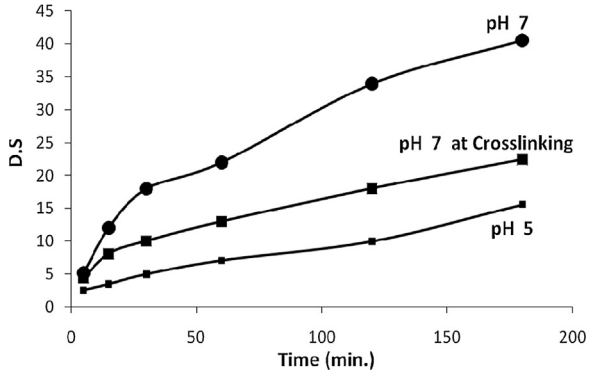

Fig. 4. The degrees of swelling of the PVA/chitosan samples, when crosslinked at pH (5, 7) and without crosslinked at pH 7 and 25 °C.

3.5. X-ray diffraction (XRD)

The XRD pattern of the crosslinked PVA/chitosan, PVA and CS is shown in Fig. 5, which showed that the amorphous nature of these materials is increasing in this order PVA/CS > PVA > CS and as a result the crystallinity structures of these materials are decreasing, where amorphous diffraction peaks at $2\theta = 21^\circ$ are indicative of the blending of PVA/chitosan.

3.6. Scanning electron microscopy (SEM)

Fig. 6 presents the SEM micrographs illustrating the morphology of the adsorbent PVA/chitosan before (A) and after (B) Mn (II) adsorption. The micrographs after adsorption of Mn (II) had their surfaces covered with irregular adhered substances, which were suspected to be the adsorbate ions, unlike the structure of the adsorbent before adsorption which had a clear plain surface. The SEM images indicate that the surface was quite rough and dense in nature and thus provide maximum surface area for the adsorption of Mn ion.

3.7. Dynamic light scattering (DLS)

DLS analysis results showed different sizes of PVA/chitosan blending detected by dynamic light scattering. DLS analysis data revealed aspect of the ball milling process of PVA/CS, which occurred with different intensities, because of the rapid aggregation of PVA/CS in water suspension. The discrepancy in the size of nanoparticles could be that the dynamic light scattering method gives the hydrodynamic diameter rather than the actual diameter of nanoparticles (Prabha et al., 2002); therefore a comparison of the particle size with other techniques as well is worth it. The mean hydrodynamic particle diameter was found to be 158.2 nm for particle size of the PVA/CS blending, as shown in Fig. 7 and Table 1. The peak of particle size distributions of the PVA/CS nanoparticles indicated that the size distribution was 158.2 nm and number percentage was 99%.

3.8. Mn (II) adsorption

The adsorption trends of Mn (II) on the PVA/CS nanoparticles in aqueous solution were investigated as a function of contact time, pH, initial manganese ion concentration, dose and different metal ion concentrations.

3.8.1. Effect of pH

In the adsorption process, the pH of solution is a very important variable that affects the metal sorption by protonation/deprotonation of the functional groups of adsorbent. Consequently, the effect of pH on the manganese onto PVA/chitosan

Table 1
DLS data of particle size distributions of the PVA/CS nanoparticles.

Size (d nm)	Mean number (%)
122.4	7.0
141.8	25.7
164.2	36.6
190.1	24.3
220.2	6.3

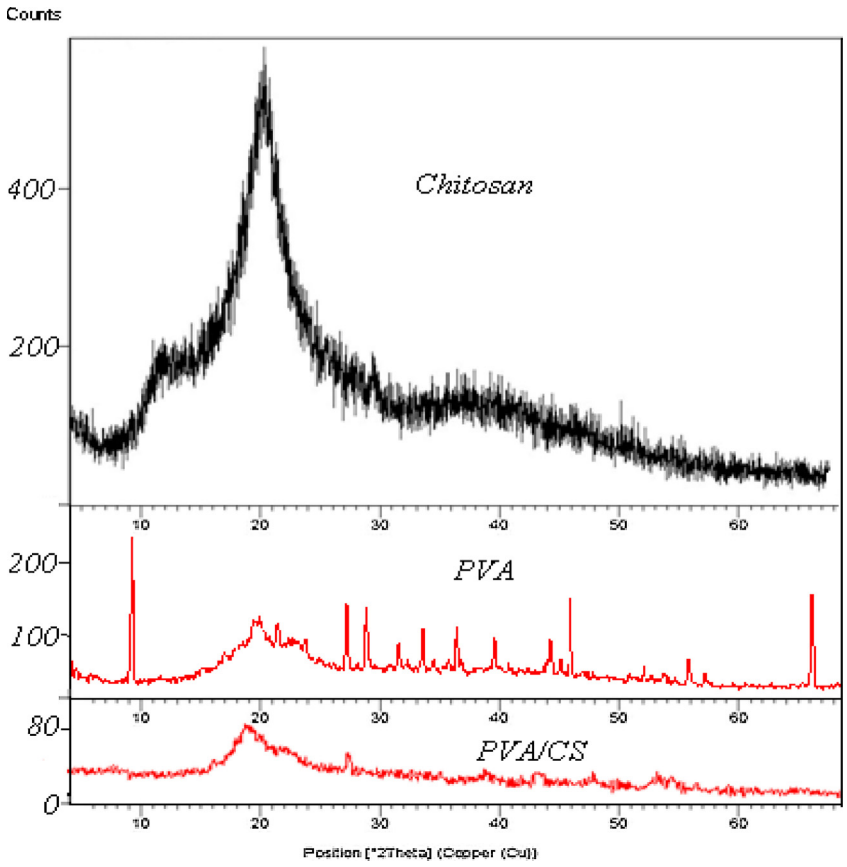

Fig. 5. XRD pattern of the chitosan, PVA and PVA/chitosan dried blending.

nanoparticles is investigated in the pH range of 2–7 for the initial concentration of 20 mg/L, adsorbent concentration 0.8 g/100 ml. The results are presented in Fig. 8. At very low pH, the concentration of H^+ ions was high. This led to the development of positive charge on the active sites of biomass and also a competition between Mn (II) ions and H^+ in the bulk of solution to attach with the active binding sites of PVA/CS. So, there was a minimum binding of Mn (II) ions at low pH. As the pH of a solution increases, PVA/CS becomes less positive and the concentration of H^+ ions also decreases. Thus, there is less competition of Mn (II) ions with H^+ ions and this resulted in more biosorption. So, it was concluded that the optimum pH for biosorption of Mn (II) ion on PVA/chitosan was 5.0.

3.8.2. *The effect of adsorbent dose*

Adsorbent dosage has a major effect on the sorption process and defines the potential of the adsorbent through the number of binding sites available to remove heavy metal ions at a specified initial concentration. The effect of adsorbent dose on the adsorption of Mn (II) has been investigated by employing different doses of PVA/CS nanoparticles varying from 0.1 to 1 g/100 ml. These adsorption experiments are performed at pH 6 and equilibrium time 2 h. Fig. 9 demonstrates the removal of Mn (II) increases with increase in adsorbent dose. With the increase in biosorbent dose of PVA/CS from 0.1 to 1.0 g/100 ml, the removal efficiency increases from 30.50 to 84.5%. This increase in the adsorption can attribute to

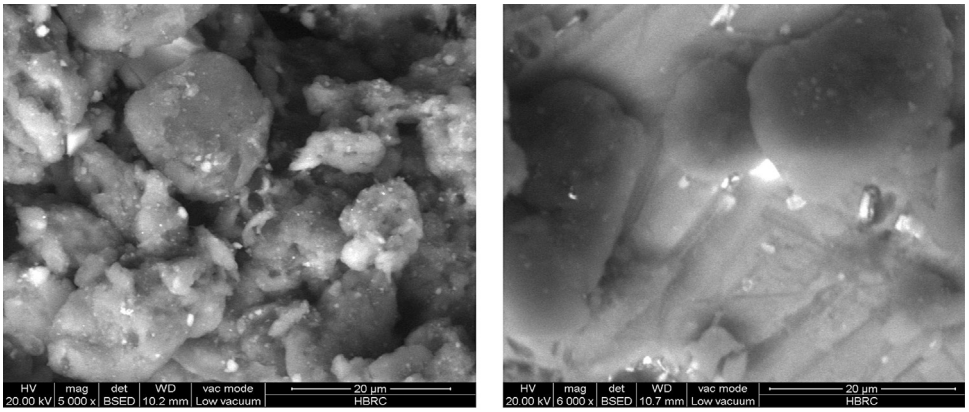

(A) (B)

Fig. 6. SEM images of the dried crosslinked PVA/chitosan (A) before and after Mn (II) adsorption (B).

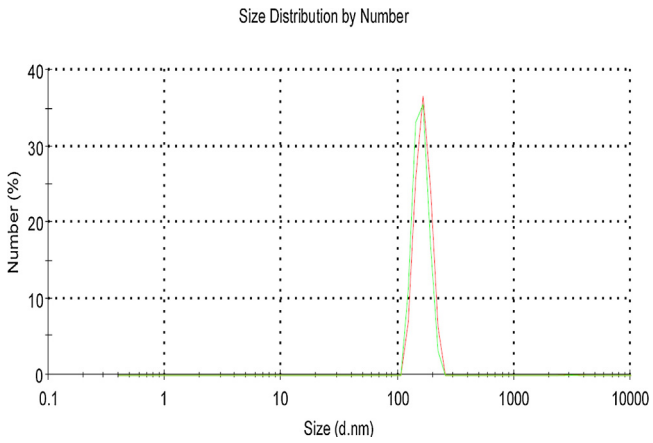

Fig. 7. Particle size distributions of the PVA/CS nanoparticles as measured by DLS.

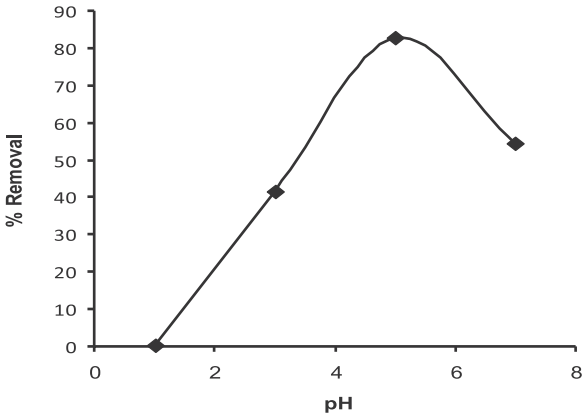

Fig. 8. Effect of pH on biosorption of Mn (II) by PVA/CS adsorbent dose 0.8 g, initial metal ion concentration 20 mg/L, temperature 30 °C.

greater surface area of PVA/CS nanoparticles and the availability of more adsorption surface sites (Saeed et al., 2010; Ahmad, 2009). It can be seen that for 20 mg/L, 0.8 g of PVA/CS in 100 ml is sufficient for the adsorption studies as it shows 83.5% removal. Similar behavior for the effect of biosorbent dose was observed for biosorption of Mn (II) ion on raw and oxalic acid modified maize husk (Abideen et al., 2013).

3.8.3. The effect of contact time

The effect of contact time on the sorption of Mn (II) ion onto the PVA/CS nanoparticles adsorbent is indicated in Fig. 10. As can be seen, the adsorption capacity shows a rapid increase during the

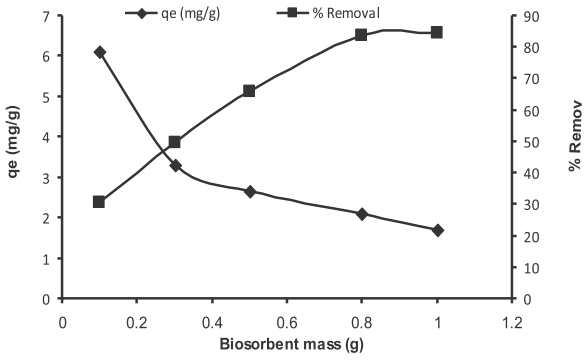

Fig. 9. Effect of biosorbent dose of Mn (II) by PVA/CS (experimental conditions: initial Mn concentration = 20 mg/L, pH 5, agitation speed = 200 rpm, contact time = 2 h at 30 °C).

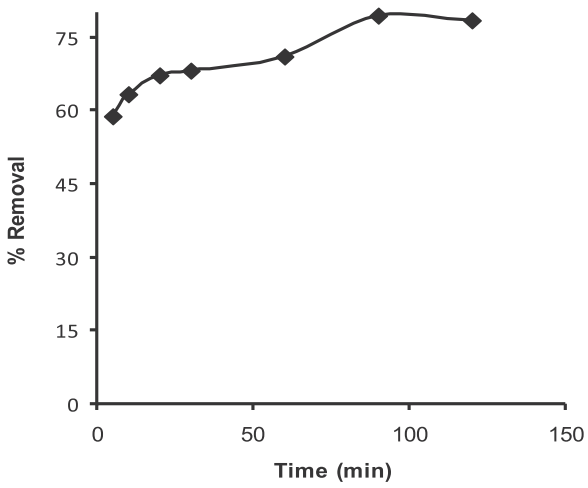

Fig. 10. Effect of contact time on Mn (II) adsorption on PVA/CS, pH = 6.0.

first period and then a slow increase follow-up until equilibrium state is reached. In general, about 80% of the total metal ion sorption was achieved within 90 min because all active sites on the adsorbent surface were vacant. Therefore, a contact time of 90 min was selected for all batch adsorption experiments.

3.8.4. Effect of different concentrations

The effect of Mn (II) concentrations on adsorption of PVA/CS nanoparticles process has been studied at pH 5 and equilibrium time of 2 h. To study the effect of initial metal ion concentrations of 5, 10, 20, 50 and 100 mg/L with PVA/CS doses of 0.8 g/100 ml shown in Fig. 11. It has been found that the biosorption capacity of the adsorbent PVA/CS increases from 0.596 to 9.225 mg/g with increasing metal ion concentrations from 5 to 100 mg/L. The initial metal ion concentration provides an important driving force to overcome all the mass transfer resistance between the solution and solid phases, and hence a higher initial concentration of metal ion may increase the biosorption capacity.

3.9. Adsorption isotherm

Analysis of adsorption equilibrium data is important for optimizing the design of an adsorption system. Adsorption isotherm expresses the relationship between metal ions adsorbed onto the adsorbents and metal ions in the solution and provides important design parameters for adsorption system. Several isotherm models have been widely used to model the equilibrium of adsorption system. Langmuir and Freundlich models are the most widely

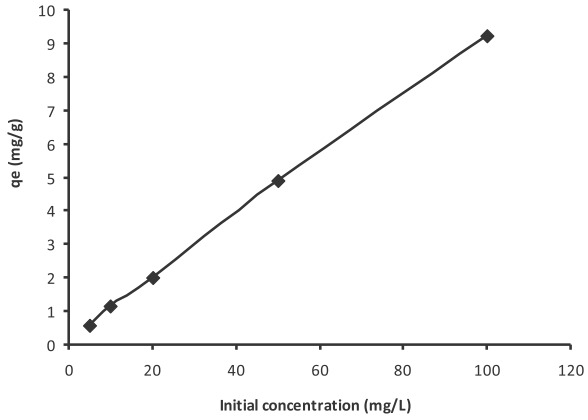

Fig. 11. Effect of initial metal ion concentrations of Mn (II) biosorption on PVA/CS.

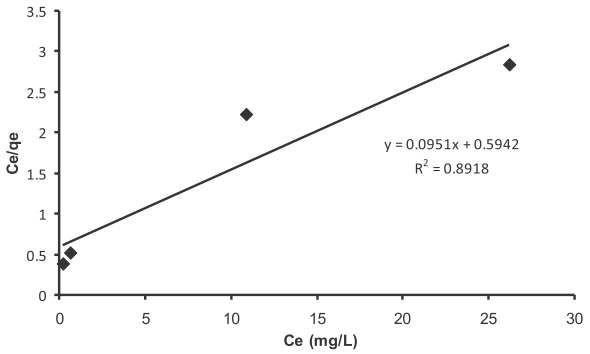

Fig. 12. Langmuir isotherm plot for adsorption of Mn (II) onto PVA/CS.

used models in the case of the adsorption of Mn (II) onto PVA/CS nanoparticles adsorbent (Fillipovic-Kovacevic et al., 2000). The Langmuir isotherm model assumes a monolayer adsorption onto a homogeneous surface where the binding sites have equal affinity and energy, and there is no interaction between molecules (Repo et al., 2010). The linear form of the Langmuir isotherm is given as:

$$\frac{C_e}{q_e} = \frac{1}{Q_m b} + \frac{C_e}{Q_m} \quad (6)$$

where Q_e (mg/g) and C_e (mg/L) are the equilibrium pollutant concentrations in the solid and liquid phase, respectively. Q_{max} (mg/g) and b (L/mg) are the Langmuir constants related to saturated monolayer adsorption capacity and the binding energy of the sorption system, respectively, Fig. 12. The Freundlich isotherm assumes that the adsorption of pollutant occurs on a heterogeneous surface by multilayer adsorption and that the amount of adsorbate adsorbed increases infinitely with an increase in concentration (Jain et al., 2009).

The linearized Freundlich isotherm is expressed as:

$$\log q_e = \frac{\log K_f + 1}{n \log C_e} \quad (7)$$

where values K_f and n are the Freundlich parameters related to the adsorption capacity and intensity of adsorption, respectively. The Freundlich isotherm model fitted the adsorption equilibrium data very well due to the heterogeneous interactions between Mn and PVA/CS nanoparticles, Fig. 13. The Langmuir and Freundlich isotherm constants together with the correlation coefficients in single system are presented in Table 2. As can be seen from Table 2, the Freundlich isotherm model gave the highest R^2 value, showing that the equilibrium data of Mn^{2+} ions on PVA/CS nanoparticles were best represented by this model. When the q_{max} value of the prepared PVA/CS adsorbent was compared with those of other adsorbents (Table 3), the adsorption capability of the PVA/CS

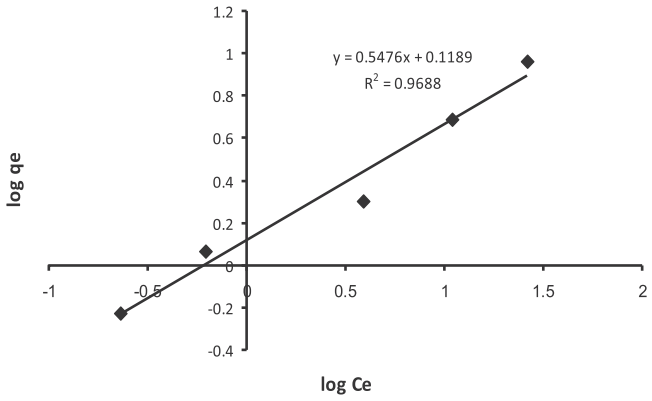

Fig. 13. Freundlich isotherm plot for adsorption of Mn (II) onto PVA/CS.

Table 2
Isotherm parameters for adsorption of Mn (II) onto PVA/CS.

Isotherm model	Parameters
Langmuir isotherm	
q_m (mg/g)	10.515
b (L/mg)	0.160
R^2	0.8918
Freundlich isotherm	
K_F (mg/g) (1 $mg^{-1})^{1/n}$	1.31
$1/n$	0.54
R^2	0.9688

Table 3
Adsorption capacities of Mn^{2+} ions by various adsorbents.

Adsorbents	q_{max} (mg/g)	Reference
Activated carbon immobilized by tannic acid	01.73	[18]
PVA/AAc hydrogels	*27.77*	[16]
PVA/CS hydrogels	10.515	This work
Crab shell particles	69.90	[17]

The italic value signifies that q_{max} is the amount of adsorbed adsorbate in unit mass of adsorbent with respect to complete monolayer coverage.

nanoparticles for Mn^{2+} ions was found to be comparable or acceptable to other adsorbents. This result reveals that the PVA/CS nanoparticles are effective adsorbents for Mn^{2+} ions from wastewater due to its low cost and friendly environmental adsorbent.

3.10. Kinetic studies

For analyzing the adsorption kinetics of heavy metal ions, the pseudo-first- and pseudo-second-order and intra-particle diffusion model were applied to the experimental data. The first-order rate equation is one of the most widely used equations for the adsorption of a solute from an aqueous solution and is represented as:

$$\log(q_e - q_t) = \log(q_e) - \frac{K_1}{2.303}(t) \quad (8)$$

where q_e and q_t are the amount of metal ion adsorbed (mg/g) at equilibrium and time t, respectively. K_1 is the first-order reaction rate constant (L/min). Examination of the data shows that the pseudo-first-order kinetic model is not applicable to Mn^{2+} ions adsorption onto PVA/CS nanoparticles judged by low correlation coefficient. The pseudo-second-order equation based on adsorption equilibrium capacity may be expressed as follows:

$$\frac{t}{q_t} = \frac{1}{K_2 q_e^2} + \frac{1}{q_e}(t) \quad (9)$$

where q_e is the equilibrium biosorption capacity and K_2 is the pseudo-second order rate constant (g/mg min). A plot of (t/q_t) versus t gives a linear relationship for the applicability of the second-order kinetic model, Fig. 14. The initial sorption rate can be calculated using the relation (Koynucu, 2008).

$$K_0 = K_2 q_e^2 \quad (10)$$

As seen from Table 4, due to high R^2, the pseudo-second order is a predominant kinetic model for the Mn (II) adsorption by PVA/CS nanoparticles. The similar kinetic result was reported for hazelnut

Table 4
Kinetic parameters for the removal of Mn (II) onto PVA/CS.

Kinetic model	Parameter	Value
Pseudo-second order	K_2 (g/mg min)	0.128
	K_0 (g/mg min)	0.520
	R^2	0.9971
	q_e (mg/g)	2.016

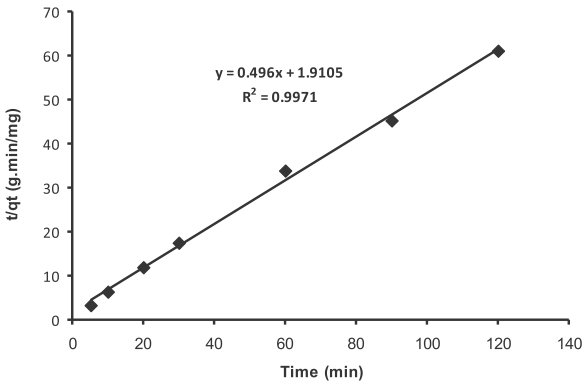

Fig. 14. Pseudo-second-order kinetic plot for the biosorption of Mn (II) onto PVA/CS at 30 °C.

shell and *Pyracantha coccinea* (Safa and Bhatti, 2011; Akar et al., 2010).

3.11. Biosorption thermodynamics

The effect of temperature on the adsorption of Mn^{2+} ions onto PVA/CS nanoparticles was studied in 298, 308, 318 and 323 K at a constant concentration of 20 mg/L, pH 6.0 and 2 h of contact time. The results showed that the adsorption capacity of Mn^{2+} ions onto PVA/CS increased with increase in temperature, indicating that the adsorption process was endothermic in nature. The thermodynamic equilibrium constant (K_d, L/g) for the adsorption of Mn^{2+} ions on PVA/CS adsorbent was calculated for all temperatures by using Eq. (10):

$$K_d = \frac{Q_e}{C_e} \tag{11}$$

Thermodynamic parameters, Gibbs free energy change (ΔG°), the enthalpy change (ΔH°) and the entropy change (ΔS°) were calculated using the following equations:

$$\ln K_d = \frac{\Delta S}{R} - \frac{\Delta H}{RT} \tag{12}$$

$$\Delta G^\circ = -RT \ln K_d \tag{13}$$

where R is the universal gas constant (8.314 J/(mol K)) and T is the absolute temperature (K). The values of ΔH° and ΔS° can be calculated from the slope and intercept of the plot of $\ln K_d$ versus $1/T$, Fig. 15, respectively. The thermodynamic parameters for the adsorption process are given in Table 5. The negative value of ΔG° at three temperatures confirms the spontaneous nature and feasibility of the biosorption process for Mn (II) onto BPAC. The

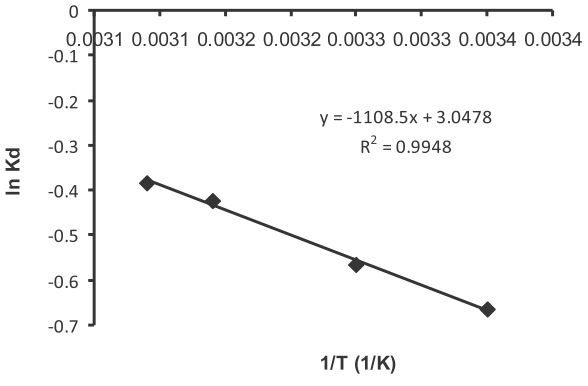

Fig. 15. Variation of $\ln K_d$ with temperature ($1/T$) for the biosorption of Mn (II) onto PVA/CS.

Table 5
Thermodynamic parameters for the adsorption of Mn (II) onto PVA/CS nanoparticles.

$-\Delta G^\circ$ (kJ/mol)				R^2	ΔH° (kJ/mol)	ΔS° (J/mol K)
298 K	308 K	318 K	323 K			
7.53	7.79	8.04	8.17	0.994	9.21	25.33

positive value of ΔH° confirms that the process is endothermic in nature. The positive value of entropy ΔS° shows increased randomness at the solid–solution interface during the biosorption process (Kelleher et al., 2002).

4. Conclusion

The preparing of polyvinyl alcohol–chitosan (PVA/CS) nanoparticles using ball milling methods and testing it as an adsorbent for removing of Mn (II) from aqueous solution were done. The batch study parameters, pH of the solution, adsorbent dose, adsorbent concentration and contact time were found to be effective on the adsorption efficiency of Mn (II). The experimental data obtained from kinetic and isotherm studies well fitted the pseudo-second-order kinetic model and Freundlich isotherm model. The thermodynamic study indicated that the adsorption of Mn (II) ion onto PVA/CS cross-linked hydrogel nanoparticles is spontaneous and endothermic in nature. The results revealed that the preparing of PVA/CS cross-linked hydrogel nanoparticles as an adsorbent for pollutants without using crosslinker and using the ball milling as a simple method is economic. In addition, due to its biodegradability, it is considered as friendly environmental adsorbent.

References

Abdeen, Z., (Ph.D. thesis) 2005. Preparations and Applications of Some Friendly Environmental Compounds. Ain Shams University, Cairo.
Abdeen, Z., 2011. Swelling and reswelling characteristics of cross-linked poly(vinyl alcohol)/chitosan hydrogel film. J. Dispers. Sci. Technol. 32 (9), 1337–1344.
Abideen, I.A., Mopelola, A.I., Andrew, E.O., Sarafadeen, O.K., Sikiru, A.A., 2013. Comparative biosorption of Mn(II) and Pb(II) ions on raw and oxalic acid modified maize husk: kinetic, thermodynamic and isothermal studies. Appl. Water Sci. 3, 167–179.
Abollino, O., Aceto, M., Malandrino, M., Sarzanini, C., Mentasti, E., 2003. Adsorption of heavy metals on Na-montmorillonite. Effect of pH and organic substances. Water Res. 37, 1619–1627.
Adeogun, A.I., Ofudje, A.E., Idowu, M.A., Kareem, S.O., 2011. Equilibrium, kinetic, and thermodynamic studies of the biosorption of Mn(II) ions from aqueous solution by raw and acid-treated corncob biomass. BioResources 6, 4117–4134.
Ahmad, R., 2009. Studies on adsorption of crystal violet dye from aqueous solution onto coniferous pinus bark powder (CPBP). J. Hazard. Mater. 171, 767–773.
Akar, T., Celik, S., Akar, S.T., 2010. Biosorption performance of surface modified biomass obtained from *Pyracantha coccinea* for the decolonization of dye contaminated solutions. Chem. Eng. J. 160 (2), 466–472.
Bailey, S.E., Olin, T.J., Bricka, R.M., Adrian, D.D., 1999. A review of potentially low-cost sorbents for heavy metals. Water Res. 33, 2469.
Berger, J., Reist, M., Mayer, J.M., Felt, O., Peppas, N.A., Gurny, R., 2004. Structure and interactions in covalently and ionically crosslinked chitosan hydrogels for biomedical applications. Eur. J. Pharm. Biopharm. 57, 19–34.
Ferrus, R., Pages, P., 1977. Water retention value and degree of crystallinity by infrared absorption spectroscopy in caustic-soda-treated cotton. Cell. Chem. Technol. 11 (6), 633–637.
Fillipovic-Kovacevic, Z., Sipos, L., Briski, F., 2000. Biosorption of Cr, Cu, Ni and Zn ions onto fungal pellets of *Asperigillus niger* 405 from aqueous solutions. Food Technol. Biotechnol. 38, 211–216.
Folkes, M.H., Hope, P.S., 1985. Polymer Blend and Alloys. Chapman and Hall, London, pp. 430–440.
Hennink, W.E., Nostrum, C.F.V., 2002. Novel crosslinking methods to design hydrogels. Adv. Drug Deliv. Rev. 54, 13–36.
Jain, M., Garg, V.K., Kadirvelu, K., 2009. Chromium(VI) removal from aqueous system using *Helianthus annuus* (sunflower) stem waste. J. Hazard. Mater. 162, 365–372.
Jin, L., Bai, R., 2002. Mechanisms of lead adsorption on chitosan/PVA hydrogel beads. Langmuir 18, 9765–9770.
Kao, W.C., Wu, J.Y., Chang, C.C., Chang, J.S., 2009. Cadmium biosorption by polyvinyl alcohol immobilized recombinant *Escherichia coli*. J. Hazard. Mater. 169, 651–658.
Kelleher, B.P., O'Callaghan, M.N., Leahy, M.J., O'Dwyer, T.F., Leahy, J.J., 2002. The use of fly ash from the combustion of poultry litter for the adsorption of chromium(III) from aqueous solution. J. Chem. Technol. Biotechnol. 77, 1212–1218.

Khoo, K.M., Ting, Y.-P., 2001. Biosorption of gold by immobilized fungal biomass. Biochem. Eng. J. 8, 51–59.
Kong, L.B., Ma, J., Huang, H., 2002. Mater. Lett. 56, 238–243.
Koynucu, H., 2008. Adsorption kinetics of 3-hydroxybenzaldehyde on native and activated bentonite. Appl. Clay Sci. 38, 279.
Kumar, M.N.V.R., 2000. A review of chitin and chitosan applications. React. Funct. Polym. 46, 1–27.
McKay, G., Blair, H.S., Gardner, J.R., 1987. Two resistance mass transport model for the adsorption of acid dye onto chitin in fixed beds. J. Appl. Polym. Sci. 33 (4), 1247–1256.
Mima, M., Mima, S., Miya, M., Iwamoto, R., Yoshikawa, S., 1983. Highly deacetylated chitosan and its properties. J. Appl. Polym. Sci. 28 (6), 1909–1917.
Miya, M., Iwamoto, R., 1984. J. Polym. Sci. Polym. Phys. Ed. 22, 1149.
Muzzarelli, R.A.A., 1977. Chitin. Pergamon Press, Oxford.
Ngah, W.S.W., Endud, C.S., Mayanar, R., 2002. Removal of copper(II) ions from aqueous solution onto chitosan and cross-linked chitosan beads. React. Funct. Polym. 50, 181–190.
Nourbakhsh, M., Illhan, S., Ozdag, H., 2002. Biosorption of Cr^{6+}, Pb^{2+} and Cu^{2+} ions in industrial wastewater on *Bacillus* sp. Chem. Eng. J. 85, 351–355.
Prabha, S., Zhou, W.-Z., Panyam, J., Labhasetwar, V., 2002. Size-dependency of nanoparticle-mediated gene transfection: studies with fractionated nanoparticles. Int. J. Pharm. 244 (1/2), 105–115.
Repo, E., Warchol, J.K., Kurniawan, T.A., Sillanpaa, M.E.T., 2010. Adsorption of Co(II) and Ni(II) by EDTA- and/or DTPA-modified chitosan: kinetic and equilibrium modeling. Chem. Eng. J. 161, 73–82.
Saeed, A., Sharif, M., Iqbal, M., 2010. Application potential of grapefruit peel as dye sorbent: kinetics, equilibrium and mechanism of crystal violet adsorption. J. Hazard. Mater. 179, 564–572.
Safa, Y., Bhatti, H.N., 2011. Kinetic and thermodynamic modeling for the removal of Direct Red-31 and Direct Orange-26 dyes from aqueous solutions by rice husk. Desalination 272 (1–3), 313–322.
Tan, O.K., Cao, W., Hu, Y., Zhu, W., 2004. Solid State Ion. 172, 309–316.
Üçer, A., Uyanik, A., Aygün, S.F., 2006. Adsorption of Cu(II), Cd(II), Zn(II), Mn(II) and Fe(III) ions by tannic acid immobilised activated carbon. Sep. Purif. Technol. 47, 113–118.
Vijayaraghavan, K., Heng Yun Ni, W., Balasubramanian, R., 2011. Biosorption characteristics of crab shell particles for the removal of manganese(II) and zinc(II) from aqueous solutions. Desalination 266, 195–200.
Xu, Y., Gallert, C., Winter, J., 2008. Chitin purification from shrimp wastes by microbial deproteination and decalcification. Appl. Microbiol. Biotechnol. 79, 687.
Yahya, H.F., Ghada, A.M., Abdel Khalek, M.A., 2014. J. Radiat. Res. Appl. Sci. 7, 135–145.
Zaluski, L., Zaluska, A., Ström-Olsen, J.O., 1995. J. Alloys Compd. 217, 245–249.